Regularized 13 Moment Equations for Rarefied Gas Flows

Henning Struchtrup[1] and Manuel Torrilhon[2]

[1] Department of Mechanical Engineering, University of Victoria, PO Box STN CSC 3055, Victoria BC V8W 3P6, Canada, struchtr@me.uvic.ca
[2] Seminar for Applied Mathematics, ETH Zürich, ETH-Zentrum, CH-8092 Zürich, Switzerland, manuel@math.ethz.ch

Summary. A new closure for Grad's 13 moment equations is presented that adds terms of super-Burnett order to the balances of pressure deviator and heat flux vector. The resulting system of equations contains the Burnett and super-Burnett equations when expanded in a series in the Knudsen number. However, other than the Burnett and super-Burnett equations, the new set of equations is linearly stable for *all* wavelengths and frequencies. Dispersion relation and damping for the new equations agree better with experimental data than those for the Navier-Stokes-Fourier equations, or the original 13 moments system. The new equations allow the description of Knudsen boundary layers, and yield smooth shock structures for all Mach numbers in good agreement with experiments and DSMC simulations.

1 Introduction

Processes in rarefied gases are well described by the Boltzmann equation [1, 2], a non-linear integro-differential equation that describes the evolution of the particle distribution function $f(\mathbf{x}, t, \mathbf{c})$ in phase space. Here $\mathbf{x}$ and t are the space and time variables, respectively, and $\mathbf{c}$ denotes the microscopic velocities of particles. The distribution function is defined such that $f(\mathbf{x}, t, \mathbf{c})\, d\mathbf{c}d\mathbf{x}$ gives the number of gas particles in the phase space cell $d\mathbf{c}d\mathbf{x}$. Thus f is a function of seven independent variables, and the numerical solution of the Boltzmann equation, either directly [3] or via the Direct Simulation Monte Carlo (DSMC) method [4], is very time expensive. In particular that is the case at low Mach numbers in the transition regime. Since this regime is important for the simulation of microscale flows, e.g. in MEMS, there is a strong desire for accurate models which allow the calculation of processes in rarefied gases at lower computational cost.

Macroscopic models can be derived form the Boltzmann equations, in particular for smaller values of the Knudsen number Kn, defined as the ratio between the mean free path of the molecules and the relevant macroscopic

length scale. In this paper we present a new model, the regularized 13 moment equations, or R13 equations [5][6], which agrees with the Boltzmann equation up to third order in the Knudsen number.

Before we discuss the new equations in some detail, we give an overview on methods to derive macroscopic equations from the Boltzmann equation. Then we introduce the R13 equations and discuss their main features.

2 Macroscopic models for rarefied gas flows

2.1 Chapman-Enskog expansion

The best known approach to derive macroscopic transport equations from the Boltzmann equation is the Chapman-Enskog method [1, 2, 7] where the distribution function is expanded in powers of the Knudsen number, $f = f^{(0)} + \mathrm{Kn} f^{(1)} + \mathrm{Kn}^2 f^{(2)} + \cdots$. The expansion parameters $f^{(\alpha)}$ are determined successively by plugging this expression into the Boltzmann equation, and equating terms with the same factors in powers of the Knudsen number, see e.g. Refs. [1, 2, 7] for details.

To zeroth order the expansion yields the Euler equations, the first order correction results in the equations of Navier-Stokes and Fourier, the second order expansion yields the Burnett equations [2, 7], and the third order expansion yields the so-called super-Burnett equations [8, 9].

The equations of Navier-Stokes and Fourier cease to be accurate for Knudsen numbers above 0.05, and one is lead to think that Burnett and super-Burnett equations are valid for larger Knudsen numbers. Unfortunately, however, the higher order equations become linearly unstable for processes involving small wavelengths, or high frequencies [8], and they lead to unphysical oscillations in steady state processes [10], and thus cannot be used in numerical simulations .

There is no clear argument why the Chapman-Enskog expansion leads to unstable equations. It seems, however, that a first order Chapman-Enskog expansion leads generally to stable equations, while higher order expansions generally yield unstable equations, although exceptions apply, e.g. see [11][12].

In recent years, several authors presented modifications of the Burnett equations that contain additional terms of Super-Burnett order (but not the actual super-Burnett terms) to stabilize the equations to produce the "augmented Burnett equations" [13][14], or derived regularizations of hyperbolic equations that reproduce the Burnett equations when expanded in the Knudsen number [15, 16]. These models are only partially successful: the augmented Burnett equations still are unstable in space [6], and both approaches lack a rational derivation from the Boltzmann equation [6].

2.2 Grad's moment method

In the method of moments of Grad [17, 18], the Boltzmann equation is replaced by a set of moment equations, - first order partial differential equations for the moments of the distribution function. Which and how many moments are needed depends on the particular process, but experience shows that the number of moments must be increased with increasing Knudsen number [19, 20, 21, 22, 23].

For the closure of the equations, the phase density is approximated by an expansion in Hermite polynomials about the equilibrium distribution (the local Maxwellian), where the coefficients are related to the moments.

Only few moments have an intuitive physical meaning, i.e. density ϱ, momentum density ϱv_i, energy density ϱe, heat flux q_i and pressure tensor p_{ij}. This set of 13 moments forms the basis of Grad's well known 13 moment equations [17] which are commonly discussed in textbooks. However, the 13 moment set does not allow the computation of boundary layers [24, 25, 20] and, since the equations are symmetric hyperbolic, leads to shock structures with discontinuities (sub-shocks) for Mach numbers above 1.65 [19, 26]. With increasing number of moments, one can compute Knudsen boundary layers [27, 20, 28] and smooth shock structures up to higher Mach numbers [26, 22]. As becomes evident from the cited literature, for some problems, in particular for large Mach or Knudsen numbers, one has to face hundreds of moment equations.

2.3 Reinecke-Kremer-Grad method

In most of the available literature, both methods - moment method and Chapman-Enskog expansion - are treated as being completely unrelated. However, using a method akin to the Maxwellian iteration of Truesdell and Ikenberry [29, 30], Reinecke and Kremer could extract the Burnett equations from Grad-type moment systems [31, 32].

Which set of moments one has to use for this purpose depends on the model for the collisions of particles. For Maxwell molecules it is sufficient to consider Grad's classical set of 13 moments.

In Ref. [25] it was shown that this iteration method is equivalent to the Chapman-Enskog expansion of the moment equations. In the original Chapman-Enskog method one first expands, and then integrates the resulting distribution function to compute its moments. In the Reinecke-Kremer-Grad method, the order of integration and expansion is exchanged.

2.4 Regularization of Grad's 13 moment equations

The original derivation of the regularized 13 moment equations uses a different combination of the methods of Grad and Chapman-Enskog. The basic idea is to assume different time scales for the 13 basic variables of the theory on one

side, and all higher moments on the other. Under that assumption, one can perform a Chapman-Enskog expansion around a non-equilibrium state which is defined through the 13 variables.

This idea was also presented by Karlin et al. [33] for the linearized Boltzmann equation. Based on the above idea they compute an approximation to the distribution function, which they then use to derive a set of 13 linear equations for the 13 moments. These equations correspond to Grad's 13 moment equations for linear processes plus some additional terms.

Our derivation of the R13 equations in Ref. [5] exchanges the order of expansion and integration: The derivation of the equations is based on the non-linear moment equations for 26 moments, instead of the linearized Boltzmann equation, so that we obtain a set of *non-linear* equations. Also, the use of moment equations allows for a much faster derivation of the equations, and yields explicit numerical expressions for coefficients that were not specified in Ref. [33]. The Karlin et al. equations follow from our equations by linearization.

A closer inspection of the regularized equations shows that the terms added to the original Grad equations are of super-Burnett order. The additional terms, which are obtained from the moment equations for higher moments, place the new equations in between the Super-Burnett and Grad's 13 moment equations in as much as the new equations keep the desirable features of both, while discarding the unwelcome features.

In particular, the R13 equations

- contain the Burnett and Super-Burnett equations as can be seen by means of a Chapman-Enskog expansion in the Knudsen number,
- are linearly stable for all wavelengths, and/or frequencies,
- show phase speeds and damping coefficients that match experiments better than those for the Navier-Stokes-Fourier equations, or the original 13 moments system,
- exhibit Knudsen boundary layers,
- lead to smooth shock structures for all Mach numbers.

The most important of these features will be discussed in the sequel.

Hyperbolic partial differential equations imply finite wave speeds and discontinuities that make them difficult to handle with standard analysis. Regularization is a method to add some parabolic terms which change the character of the equations so that no discontinuities occur, but a narrow smooth transition zone [34, 35]. We decided to adopt the notion of regularization for the new equations since the additional terms indeed are smoothing out the discontinuities (sub-shocks) that occur in Grad's 13 moment system for Mach numbers above 1.65. It is important to note, though, that the shocks in Grad's moment equations (at $\mathrm{Ma} = 1.65$ for 13 moments, at higher Mach numbers for extended moment sets, see Refs. [26]) are artefacts of the method, and thus unphysical. The parameter that controls our regularization is the mean time of free flight, which is a physical parameter. In other words, the regularization

of Grad's 13 moment system removes artificial discontinuities, and replaces them by a shock structure which is based in physics.

2.5 Order of magnitude / order of accuracy approach

The weak point in the derivation of the R13 equations as outlined above is the assumption of different time scales for the basic 13 moments, and higher moments. While this assumption leads to a set of equations with desired behavior, it is difficult to justify, since the characteristic times of all moments are of the same order.

Only recently, an alternative approach to the problem was presented by Struchtrup in Ref. [36]. This approach is an extension of an idea developed by Müller et al. in Ref. [37].

Müller et al. [37] consider the infinite system of coupled moment equations of the BGK equation [38]. From these they determine—by means of a Maxwell iteration—the *order of magnitude* of moments in terms of orders in powers of the Knudsen number, and then declare that a theory of order n needs to consider all moments of that order, and their respective moment equations. This approach depends strongly on the definition of moments—Müller et al. used eigenfunctions of the Boltzmann collision term for Maxwell molecules—and demands very high moment numbers already at low orders [37].

The extension of this idea in Ref. [36] is independent of the definition of moments, and yields smaller moment numbers for a theory of a given order. The main difference to the method of Ref. [37] is the distinction between the *order of magnitude* of moments, and the *order of accuracy* of the corresponding equations, both measured in powers of the Knudsen number—this difference was ignored in Ref. [37]. This method was applied to the special cases of Maxwell molecules and the BGK model, and it could be shown that it yields the Euler equations at zeroth order, the Navier-Stokes-Fourier equations at second order, Grad's 13 moment equations (with omission of a nonlinear term) at second order, and the regularized 13 moment equations in third order.

The lone scaling parameter in this method is the Knudsen number, and the assumption of different time scales is not needed for the derivation of the R13 equations. Thus, one can consider this derivation of the R13 equations to be better founded than the original derivation in Ref. [5].

3 Regularized 13 moment equations

The regularized 13 moment equations for monatomic gases were derived in [5][36], and here we just present the results. The R13 equations are a set of field equations for the 13 variables $\rho_A = \left\{\varrho, \varrho v_i, \varrho\varepsilon = \frac{3}{2}\varrho RT, \sigma_{ij}, q_i\right\}$, where ϱ is the mass density, v_i is the gas velocity, ε is the specific internal energy, T is the temperature, R is the specific gas constant, σ_{ij} is the trace-free part

of the pressure tensor, and q_i is the heat flux vector. The field equations for these variables are the conservation laws for mass, momentum and energy,

$$\begin{aligned}
\frac{\partial \rho}{\partial t} + \frac{\partial \varrho v_k}{\partial x_k} &= 0 \,, \\
\frac{\partial \rho v_i}{\partial t} + \frac{\partial}{\partial x_k}\left(\rho v_i v_k + p\delta_{ik} + \sigma_{ik}\right) &= 0 \,, \\
\frac{\partial}{\partial t}\left(\rho\varepsilon + \frac{1}{2}\rho v_i^2\right) + \frac{\partial}{\partial x_k}\left(\rho\varepsilon v_k + \frac{1}{2}\rho v_i^2 v_k + p v_k + \sigma_{ik} v_i + q_k\right) &= 0 \,,
\end{aligned} \tag{1}$$

plus additional field equations for stress deviator

$$\frac{\partial \sigma_{ij}}{\partial t} + \frac{\partial \sigma_{ij} v_k}{\partial x_k} + \frac{4}{5}\frac{\partial q_{\langle i}}{\partial x_{j\rangle}} + 2p\frac{\partial v_{\langle i}}{\partial x_{j\rangle}} + 2\sigma_{k\langle i}\frac{\partial v_{j\rangle}}{\partial x_k} + \frac{\partial m_{ijk}}{\partial x_k} = -\frac{p}{\mu}\sigma_{ij}, \tag{2}$$

and heat flux

$$\begin{aligned}
&\frac{\partial q_i}{\partial t} + \frac{\partial q_i v_k}{\partial x_k} + \frac{5}{2}pR\frac{\partial T}{\partial x_i} + \frac{5}{2}\sigma_{ik}R\frac{\partial T}{\partial x_k} + RT\frac{\partial \sigma_{ik}}{\partial x_k} - \sigma_{ik}RT\frac{\partial \ln \varrho}{\partial x_k} - \frac{\sigma_{ij}}{\varrho}\frac{\partial \sigma_{jk}}{\partial x_k} \\
&+ \frac{7}{5}q_k\frac{\partial v_i}{\partial x_k} + \frac{2}{5}q_k\frac{\partial v_k}{\partial x_i} + \frac{2}{5}q_i\frac{\partial v_k}{\partial x_k} + \frac{1}{2}\frac{\partial R_{ik}}{\partial x_k} + \frac{1}{6}\frac{\partial \Delta}{\partial x_i} + m_{ijk}\frac{\partial v_j}{\partial x_k} = -\frac{2}{3}\frac{p}{\mu}q_i.
\end{aligned} \tag{3}$$

Here, $p = \varrho RT$ is the pressure, and μ denotes the viscosity. Indices in angular brackets denote the symmetric trace-free parts of tensors. The above equations contain the additional quantities m_{ijk}, R_{ik} , Δ, and constitutive equations are required to close the equations. With the choice

$$m_{ijk} = R_{ik} = \Delta = 0 \tag{4}$$

the above set of equations is reduced to the well-known set of 13-moment-equations of Grad [17][18]. The regularization of the Grad equations yields

$$\begin{aligned}
m_{ijk} &= -2\frac{\mu}{p}\left[RT\frac{\partial \sigma_{\langle ij}}{\partial x_{k\rangle}} - RT\sigma_{\langle ij}\frac{\partial \ln \varrho}{\partial x_{k\rangle}} + \frac{4}{5}q_{\langle i}\frac{\partial v_j}{\partial x_{k\rangle}} - \frac{\sigma_{\langle ij}}{\varrho}\frac{\partial \sigma_{k\rangle l}}{\partial x_l}\right], \\
R_{ij} &= -\frac{24}{5}\frac{\mu}{p}\left[RT\frac{\partial q_{\langle i}}{\partial x_{j\rangle}} + Rq_{\langle i}\frac{\partial T}{\partial x_{j\rangle}} - RTq_{\langle i}\frac{\partial \ln \varrho}{\partial x_{j\rangle}} - \frac{1}{\rho}q_{\langle i}\frac{\partial \sigma_{j\rangle k}}{\partial x_k}\right. \\
&\quad \left. + \frac{5}{7}RT\left(\sigma_{k\langle i}\frac{\partial v_{j\rangle}}{\partial x_k} + \sigma_{k\langle i}\frac{\partial v_k}{\partial x_{j\rangle}} - \frac{2}{3}\sigma_{ij}\frac{\partial v_k}{\partial x_k}\right) - \frac{5}{6}\frac{\sigma_{ij}}{\varrho}\frac{\partial q_k}{\partial x_k} - \frac{5}{6}\frac{\sigma_{ij}}{\varrho}\sigma_{kl}\frac{\partial v_k}{\partial x_l}\right], \\
\Delta &= -12\frac{\mu}{p}\left[RT\frac{\partial q_k}{\partial x_k} + \frac{5}{2}Rq_k\frac{\partial T}{\partial x_k} - RTq_k\frac{\partial \ln \varrho}{\partial x_k} + RT\sigma_{ij}\frac{\partial v_i}{\partial x_j} - \frac{1}{\varrho}q_j\frac{\partial \sigma_{jk}}{\partial x_k}\right].
\end{aligned} \tag{5}$$

In the resulting system (1)-(3) with (5), second order derivatives appear in the balance equations of stress tensor and heat flux which lead to a regularization of the original 13 moment case of Grad.

The R13 equations were derived from the Boltzmann equations for the special case of Maxwell molecules, that is particles that interact in a repulsive 5-th power potential. The corresponding viscosity is proportional to temperature as

$$\mu = \mu_0 \left(\frac{T}{T_0}\right)^s \tag{6}$$

with $s = 1$. It is well known [4] that the viscosity is of this form also for other interaction potentials if one only adjusts the exponent s. In particular one computes $s = 1/2$ for hard spheres, and one measures $s \approx 0.8$ for argon. For the purpose of this paper we shall use $s = 1$ exclusively.

4 Chapman-Enskog expansions

The idea of the Chapman-Enskog expansion is to expand the distribution function in a series in the Knudsen number Kn as

$$f = f^{(0)} + \mathrm{Kn} f^{(1)} + \mathrm{Kn}^2 f^{(2)} + \mathrm{Kn}^3 f^{(3)} + \cdots$$

where the $f^{(\alpha)}$ are obtained from the Boltzmann equation [7][2]. In our case, we operate on the level of moments and moment equations, and thus we expand pressure deviator and heat flux in a series as

$$\begin{aligned}\sigma_{ij} &= \sigma_{ij}^{(0)} + \mathrm{Kn}\sigma_{ij}^{(1)} + \mathrm{Kn}^2\sigma_{ij}^{(2)} + \mathrm{Kn}^3\sigma_{ij}^{(3)} + \cdots \\ q_i &= q_i^{(0)} + \mathrm{Kn} q_i^{(1)} + \mathrm{Kn}^2 q_i^{(2)} + \mathrm{Kn}^3 q_i^{(3)} + \cdots\end{aligned}$$

In order to expand properly, one needs to consider the dimensionless forms of equations (2) and (3), into which the above expressions are inserted. Then terms with equal powers in Kn are equated to find the $\sigma_{ij}^{(\alpha)}$, $q_i^{(\alpha)}$. Note that the dimensionless equations have $\mathrm{Kn}\mu$ instead of μ in Eqs. (2, 3, 5). The dimensions are restored after the expansion is performed.

In the Chapman-Enskog method it is customary to express the time derivatives of $\sigma_{ij}^{(\alpha)}$, $q_i^{(\alpha)}$ by time derivatives of the hydrodynamic variables ϱ, T, v_i. Some details how this must be done successively can be found for the linear case in [5], and for the non-linear case in [25].

From the R13 equations as given above we find the Euler equations at zeroth order,

$$\sigma_{ij}^{(0)} = q_i^{(0)} = 0, \tag{7}$$

and the first order corrections are the Navier-Stokes-Fourier equations

$$\sigma_{ij}^{(1)} = -2\mu \frac{\partial v_{\langle i}}{\partial x_{j\rangle}} \quad \text{and} \quad q_i^{(1)} = -\frac{15}{4} R\mu \frac{\partial T}{\partial x_i}. \tag{8}$$

The second order terms yield the Burnett equations for Maxwell molecules, that can be written as

$$\sigma_{ij}^{(2)} = \frac{\mu^2}{p}\left[R\frac{\partial^2 T}{\partial x_{\langle i}\partial x_{j\rangle}} - 2\frac{RT}{\varrho}\frac{\partial^2 \varrho}{\partial x_{\langle i}\partial x_{j\rangle}} + 2\frac{RT}{\varrho^2}\frac{\partial \varrho}{\partial x_{\langle i}}\frac{\partial \varrho}{\partial x_{j\rangle}} - 2\frac{R}{\varrho}\frac{\partial T}{\partial x_{\langle i}}\frac{\partial \varrho}{\partial x_{j\rangle}} \right.$$
$$\left. +3\frac{R}{T}\frac{\partial T}{\partial x_{\langle i}}\frac{\partial T}{\partial x_{j\rangle}} + \frac{10}{3}S_{ij}\frac{\partial v_k}{\partial x_k} - 4S_{k\langle i}\frac{\partial v_k}{\partial x_{j\rangle}} - 2\frac{\partial v_k}{\partial x_{\langle i}}\frac{\partial v_{j\rangle}}{\partial x_k} + 8S_{k\langle i}S_{j\rangle k}\right] \quad (9)$$

and

$$q_i^{(2)} = \frac{\mu^2}{p}\left[-\frac{13}{4}RT\frac{\partial^2 v_k}{\partial x_i \partial x_k} + \frac{3}{2}RT\frac{\partial^2 v_i}{\partial x_k \partial x_k} - 3\frac{RT}{\varrho}S_{ij}\frac{\partial \varrho}{\partial x_j}\right.$$
$$\left. -\frac{25}{8}R\frac{\partial v_k}{\partial x_k}\frac{\partial T}{\partial x_i} + \frac{15}{8}R\frac{\partial v_k}{\partial x_i}\frac{\partial T}{\partial x_k} + \frac{105}{8}R\frac{\partial v_i}{\partial x_k}\frac{\partial T}{\partial x_k}\right], \quad (10)$$

where we have used the abbreviation

$$S_{ij} = \frac{\partial v_{\langle i}}{\partial x_{j\rangle}}.$$

It is not surprising that the Burnett equations arise from the second order expansion of the R13 equations, since it is an established fact that the Burnett equations can be obtained already from Grad's 13-moment-equations [31][32][25], i.e. with the Grad closure (4).

Indeed, a closer inspection of the closure relations (5) of the R13 equations shows that these contribute terms of super-Burnett order. The derivation of the super-Burnett equations is a very cumbersome task, and they are quite difficult to find in the literature. Thus, we expanded the R13 equations for two special cases only: The three-dimensional, linear equations and the one-dimensional, non-linear equations. For the three-dimensional, linear case one obtains [5]

$$\sigma_{ij}^{(3)} = \frac{\mu^3}{p^2}\left(\frac{5}{3}RT\frac{\partial^2}{\partial x_{\langle i}\partial x_{j\rangle}}\frac{\partial v_k}{\partial x_k} - \frac{4}{3}RT\frac{\partial^2}{\partial x_k \partial x_k}\frac{\partial v_{\langle i}}{\partial x_{j\rangle}}\right),$$
$$q_i^{(3)} = \frac{\mu^3}{p^2}\left(-\frac{157}{16}RT\frac{\partial^3 \theta}{\partial x_i \partial x_k \partial x_k} - \frac{5}{8}\frac{R^2T^2}{\rho}\frac{\partial^3 \varrho}{\partial x_i \partial x_k \partial x_k}\right). \quad (11)$$

These are the same equations that Shavaliyev found from the Boltzmann equation [9]. It can also be shown that the third order Chapman-Enskog expansion of the non-linear one-dimensional R13 equations agrees with the corresponding super-Burnett equations [6], but we abstain from printing these here.

From the above discussion follows that the R13 equations agree up to the super-Burnett order with the Boltzmann equation. Note that Grad's classical 13 moment equations agree up to Burnett order, but not to super-Burnett order.

Moreover, the R13 equations have several advantages above the Burnett and super-Burnett equations: (a) They can be derived much easier, and faster,

so that errors can be excluded with higher certainty. (b) The R13 equations contain only space derivatives of first and second order while the super-Burnett equations contain derivatives of up to fourth order. Thus, the R13 equations fit more conveniently to existing numerical methods. Note that their mathematical structure is very similar to the NSF equations, so that methods for these can be used as well for solving the R13 equations. (c) Most important, however, is the fact that the R13 equations are linearly stable as will be shown below [5], while the Burnett and super-Burnett equations are linearly unstable [8][10].

5 Linear Stability

We start our analysis of the R13 equations by considering the linear stability. For this, we consider small deviations from an equilibrium state given by $\varrho_0, T_0, v_{i,0} = 0$, and consider one-dimensional processes where $x_1 = x$, and $v_i = \{v(x,t), 0, 0\}$. Dimensionless variables $\hat{\varrho}$, $\hat{T}$, $\hat{v}$, $\hat{\sigma}$, $\hat{q}$ are introduced as

$$\varrho = \varrho_0 (1 + \hat{\varrho}) \ , \quad T = T_0 \left(1 + \hat{T}\right) \ , \quad p = \varrho_0 R T_0 \left(1 + \hat{\varrho} + \hat{T}\right) \ ,$$
$$v = \sqrt{RT_0}\hat{v} \ , \quad \sigma_{11} = \varrho_0 R T_0 \hat{\sigma} \ , \quad q_1 = \varrho_0 \sqrt{RT_0}^3 \hat{q} \ .$$

Moreover, we identify a relevant length scale L of the process, and use it to non-dimensionalize the space and time variables according to

$$x = L\hat{x} \ , \quad t = \frac{L}{\sqrt{RT_0}}\hat{t} \ .$$

The corresponding dimensionless collision time is then given by the Knudsen number, which we define here as

$$\mathrm{Kn} = \frac{\tau\sqrt{RT_0}}{L} = \frac{\mu_0}{\varrho_0\sqrt{RT_0}L} \ .$$

Linearization in the deviations from equilibrium $\hat{\varrho}$, $\hat{T}$, $\hat{v}$, $\hat{\sigma}$, $\hat{q}$ yields the dimensionless linearized system in one dimension as

$$\begin{aligned}
\frac{\partial\hat{\varrho}}{\partial\hat{t}} + \frac{\partial\hat{v}}{\partial\hat{x}} &= 0 \ , \\
\frac{\partial\hat{v}}{\partial\hat{t}} + \frac{\partial\hat{\varrho}}{\partial\hat{x}} + \frac{\partial\hat{T}}{\partial\hat{x}} + \frac{\partial\hat{\sigma}}{\partial\hat{x}} &= 0 \ , \\
\frac{3}{2}\frac{\partial\hat{T}}{\partial\hat{t}} + \frac{\partial\hat{q}}{\partial\hat{x}} + \frac{\partial\hat{v}}{\partial\hat{x}} &= 0 \ , \\
\frac{\partial\hat{\sigma}}{\partial\hat{t}} + \frac{8}{15}\frac{\partial\hat{q}}{\partial\hat{x}} + \frac{4}{3}\frac{\partial\hat{v}}{\partial\hat{x}} - \frac{6}{5}\mathrm{Kn}\frac{\partial^2\hat{\sigma}}{\partial\hat{x}^2} &= -\frac{\hat{\sigma}}{\mathrm{Kn}} \ , \\
\frac{\partial\hat{q}}{\partial\hat{t}} + \frac{5}{2}\frac{\partial\hat{T}}{\partial\hat{x}} + \frac{\partial\hat{\sigma}}{\partial\hat{x}} - \frac{18}{5}\mathrm{Kn}\frac{\partial^2\hat{q}}{\partial\hat{x}^2} &= -\frac{2}{3}\frac{\hat{q}}{\mathrm{Kn}} \ .
\end{aligned} \tag{12}$$

This set of equations is equivalent to the equations proposed by Karlin et al. [33], who, however, did not give explicit numerical expressions for the factors that multiply the second derivatives of $\hat{\sigma}$ and $\hat{q}$, but presented them as integrals over the linearized collision operator which are not further evaluated.

For comparison, we shall also consider the Chapman-Enskog expansion to various orders (7-10), in which case we have to replace the last two equations with the relevant terms of

$$\hat{\sigma}_{CE} = -\mathrm{Kn}\frac{4}{3}\frac{\partial \hat{v}}{\partial \hat{x}} - \mathrm{Kn}^2\left[\frac{4}{3}\frac{\partial^2 \hat{\varrho}}{\partial \hat{x}^2} - \frac{2}{3}\frac{\partial^2 \hat{T}}{\partial \hat{x}^2}\right] + \mathrm{Kn}^3\frac{2}{9}\frac{\partial^3 \hat{v}}{\partial \hat{x}^3} + \cdots ,$$

$$\hat{q}_{CE} = -\mathrm{Kn}\frac{15}{4}\frac{\partial \hat{T}}{\partial \hat{x}} - \mathrm{Kn}^2\frac{7}{4}\frac{\partial^2 \hat{v}}{\partial \hat{x}^2} - \mathrm{Kn}^3\left[\frac{157}{16}\frac{\partial^3 \hat{T}}{\partial \hat{x}^3} + \frac{5}{8}\frac{\partial^3 \hat{\varrho}}{\partial \hat{x}^3}\right] + \cdots .$$

We assume plane wave solutions of the form

$$\phi = \tilde{\phi}\exp\left\{i\left(\omega\hat{t} - k\hat{x}\right)\right\}$$

where $\tilde{\phi}$ is the complex amplitude of the wave, ω is its frequency, and k is its wave number. The equations can be written as

$$\mathcal{A}_{AB}\left(\omega, k\right)\tilde{u}_B = 0 \quad \text{with} \quad \tilde{u}_B = \left\{\tilde{\varrho}, \tilde{T}, \tilde{v}, \tilde{\sigma}, \tilde{q}\right\}$$

and nontrivial solutions require

$$\det\left[\mathcal{A}_{AB}\left(\omega, k\right)\right] = 0 ,$$

the resulting relation between ω and k is the dispersion relation.

If a disturbance in space is considered, the wave number k is real, and the frequency is complex, $\omega = \omega_r\left(k\right) + i\omega_i\left(k\right)$. Phase velocity v_{ph} and damping α of the corresponding waves are given by

$$v_{ph} = \frac{\omega_r\left(k\right)}{k} \quad \text{and} \quad \alpha = \omega_i\left(k\right)$$

Stability requires damping, and thus $\omega_i\left(k\right) \geq 0$.

If a disturbance in time at a given location is considered, the frequency ω is real, while the wave number is complex, $k = k_r\left(\omega\right) + ik_i\left(\omega\right)$. Phase velocity v_{ph} and damping α of the corresponding waves are given by

$$v_{ph} = \frac{\omega}{k_r\left(\omega\right)} \quad \text{and} \quad \alpha = -k_i\left(\omega\right) .$$

For a wave traveling in positive x-direction ($k_r > 0$), the damping must be negative ($k_i < 0$), while for a wave traveling in negative x-direction ($k_r < 0$), the damping must be positive ($k_i > 0$).

It is convenient to chose the mean free path as reference length, and the mean free time as reference time, so that $\mathrm{Kn} = 1$. Then the wave number is

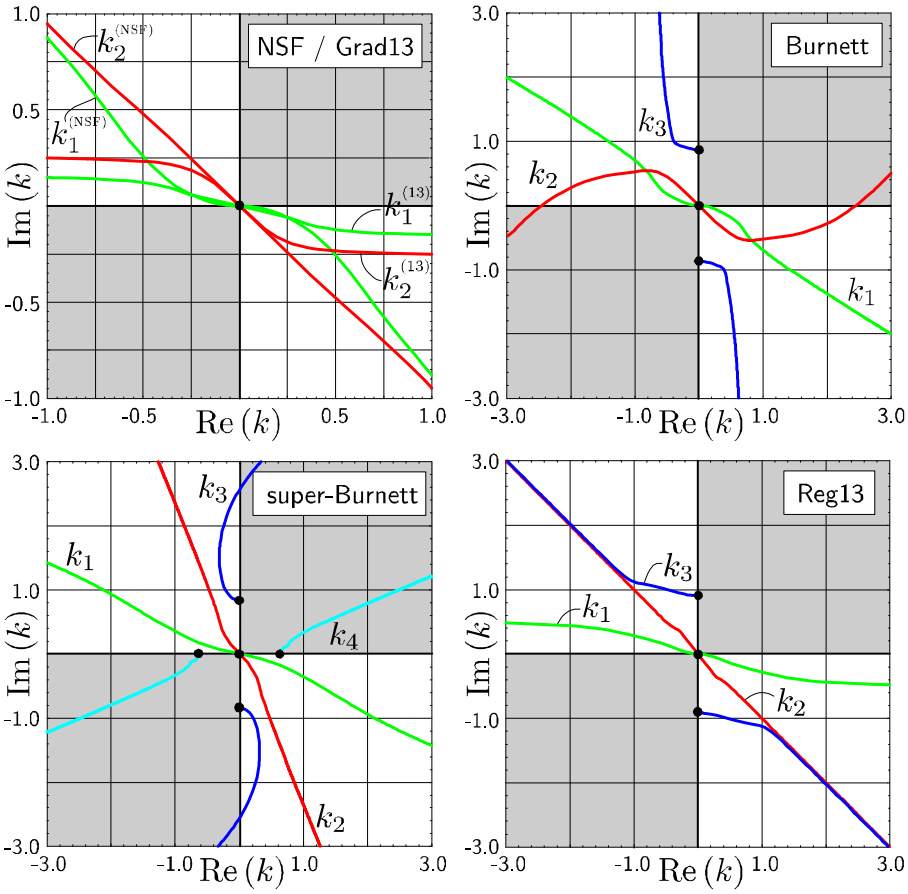

Fig. 1. The solutions $k(\omega)$ of the dispersion relation in the complex plane with ω as parameter for Navier-Stokes-Fourier, Grad's 13 moments, Burnett, Super-Burnett, and Reguarized 13 moment equations. The dots denote the points where $\omega = 0$.

measured in units of the inverse mean free path, and the wave frequency in terms of the collision frequency $1/\tau$. This implies that the Knudsen number for an oscillation with dimensionless frequency ω is $\mathrm{Kn}_\omega = \omega$, and for a given wave number k the Knudsen number is $\mathrm{Kn}_k = k$.

We test the stability against local disturbances of frequency ω. As we have seen, stability requires different signs of real and imaginary part of $k(\omega)$. Thus, if $k(\omega)$ is plotted in the complex plane with ω as parameter, the curves should not touch the upper right nor the lower left quadrant.

Fig. 1 shows the solutions for the different sets of equations considered in this paper, the dots mark the points where $\omega = 0$. Grad's 13 moment equations (Grad13), and Navier-Stokes-Fourier equations (NSF) give two different

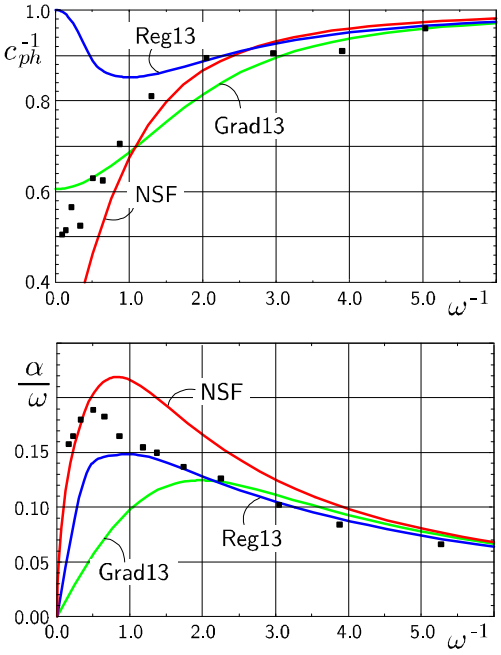

Fig. 2. Inverse phase velocity (up) and damping (below), theoretical results from Navier-Stokes-Fourier, Grad's 13 moments, and regularized 13 moments and measurements by Meyer and Sessler [39] (dots).

modes each, and none of the solutions violates the condition of stability (upper left in Fig.1). This is different for the Burnett (3 modes, upper right) and Super-Burnett (4 modes, lower left) equations: the Burnett equations have one unstable mode, and the Super-Burnett have two unstable modes. The R13 equations, shown in the lower right, have 3 modes, all of them are stable.

In a similar manner it can be shown that the R13 equations are stable with respect to a disturbance of given wave length, or wave number k, while the Burnett and Super-Burnett equations are unstable [5][8].

6 Dispersion and Damping

Next we compare phase speed and damping with experiments performed by Meyer and Sessler [39]. Fig. 2 shows the inverse phase speed and the damping (as α/ω) as functions of the dimensionless inverse frequency $1/\omega$, computed with NSF, Grad 13, and R13 equations, and experimental data from Ref. [39]. Here we consider only those modes that yield the speed of sound for $\omega \to 0$.

As can be seen, the R13 equations reproduce the measured values of the damping coefficient α for all dimensionless frequencies less than unity, while

the NSF and Grad13 equations fail already at $\omega = 0.25$ and $\omega = 0.5$, respectively. The agreement of the R13 prediction for the phase velocity is less striking, but also the other theories do not match well. One reason for this might be insufficient accuracy of the measurement. Altogether, the R13 equations give a remarkably good agreement with the measurements for values of $\omega < 1$.

Equations from expansions in the Knudsen number can be expected to be good only for $\mathrm{Kn} < 1$. We conclude that the R13 equations allow a proper description of processes quite close to the natural limit of their validity of $\mathrm{Kn}_\omega = 1$. It is not surprising that all theories show discrepancies to the experiments for larger frequencies. The reasonable agreement between the NSF phase speed and experiments must be seen as coincidence.

7 Knudsen boundary layers

In this section we briefly study boundary value problems for the linearized R13 equations. The goal is to show that the R13 equations lead to Knudsen boundary layers.

To this end we consider a simple steady state Couette flow problem: two infinite, parallel plates move in the $\{x_2, x_3\}$-plane with different speeds in x_2 direction. The plate distance is $L = 1$ in dimensionless units, and the plates have different temperatures. In this setting, we expect that all variables will depend only on the coordinate $x_1 = x$. Since matter cannot pass the plates, we will have $v_1 = 0$. Moreover, for symmetry reasons, there will be no fluxes in the x_3 direction, so that

$$v_i = \{0, v(x), 0\} \text{ and } q_3 = \sigma_{13} = \sigma_{23} = 0 \,.$$

Under these assumptions, the linearized R13 equations can be split into the flow problem with the equations

$$\frac{\partial v}{\partial x} + \frac{2}{5}\frac{\partial q_2}{\partial x} = -\frac{\sigma_{12}}{\mathrm{Kn}} = const \;\;,\;\; q_2 = \frac{9}{5}\mathrm{Kn}^2\frac{\partial^2 q_2}{\partial x^2} \,.$$

and the heat transfer problem, with the equations

$$\frac{5}{2}\frac{\partial T}{\partial x} + \frac{\partial \sigma_{11}}{\partial x} = -\frac{2}{3}\frac{q_1}{\mathrm{Kn}} = const \;\;,\;\; \sigma_{11} = \frac{6}{5}\mathrm{Kn}^2\frac{\partial^2 \sigma_{11}}{\partial x^2} \,,$$

Two more non-trivial equations serve to compute ϱ, and σ_{22}, viz.

$$\sigma_{22} = \mathrm{Kn}^2\left[\frac{2}{3}\frac{\partial^2\sigma_{22}}{\partial x^2} - \frac{4}{15}\frac{\partial^2\sigma_{11}}{\partial x^2}\right] \quad , \quad \frac{\partial \varrho}{\partial x} + \frac{\partial T}{\partial x} + \frac{\partial \sigma_{11}}{\partial x} = 0 \,.$$

The linear equations are easy to integrate, and we obtain the solution of the flow problem as

$$v(x) = v_0 - \sigma_{12}\frac{x}{\mathrm{Kn}} - \frac{2}{5}q_2(x) \tag{13}$$
$$\text{with} \quad q_2(x) = A\sinh\left(\sqrt{\frac{5}{9}}\frac{x-\frac{1}{2}}{\mathrm{Kn}}\right) + B\cosh\left(\sqrt{\frac{5}{9}}\frac{x-\frac{1}{2}}{\mathrm{Kn}}\right)$$

where v_0, σ_{12}, A, B are constants of integration.

The solution of the heat transfer problem reads

$$T(x) = T_0 - \frac{4}{15}q_1\frac{x}{\mathrm{Kn}} - \frac{2}{5}\sigma_{11}(x) \tag{14}$$
$$\text{with} \quad \sigma_{11}(x) = C\sinh\left(\sqrt{\frac{5}{6}}\frac{x-\frac{1}{2}}{\mathrm{Kn}}\right) + D\cosh\left(\sqrt{\frac{5}{6}}\frac{x-\frac{1}{2}}{\mathrm{Kn}}\right)$$

where T_0, q_1, C, D are constants of integration.

Thus, in order to obtain the fields of temperature and velocity between the plates, we need 8 boundary conditions. The velocities and temperatures of the two plates give only four boundary conditions, and thus additional boundary conditions are required. As of now, the problem how to prescribe meaningful boundary conditions for the R13 equations is unsolved, and we hope to be able to present proper boundary conditions (that, of course, allow for temperature jumps and velocity slips) in the future.

Nevertheless, it is worthwhile to study the general solutions (13, 14): In the linear Navier-Stokes-Fourier case both, temperature and velocity, are straight lines according to

$$v_{NSF}(x) = v_0 - \sigma_{12}\frac{x}{\mathrm{Kn}} \quad \text{and} \quad T_{NSF}(x) = T_0 - \frac{4}{15}q_1\frac{x}{\mathrm{Kn}}\,,$$

that is for the NSF case one finds $q_2(x) = \sigma_{11}(x) = 0$.

With the R13 equations, on the other hand, these functions are non-zero as given in (13, 14). From that, we identify $-\frac{2}{5}q_2(x)$ and $-\frac{2}{5}\sigma_{11}(x)$ as the Knudsen boundary layers for velocity and temperature according to the R13 equations. Indeed, these functions have the typical shape of a boundary layer, their largest values are found at the walls, and the curves decrease to zero within several mean free paths away from the walls.

The curves are governed by the Knudsen number, so that for small Knudsen numbers $q_2(x)$ and $\sigma_{11}(x)$ are equal to zero almost everywhere between the plates. The boundary layers are confined to a small region adjacent to the wall, and contribute to temperature jump and velocity slip. In this case, the Navier-Stokes-Fourier theory can be used with proper jump and slip boundary conditions.

As Kn grows, the width of the boundary layers is growing as well. For Knudsen numbers above $\sim$0.05 one cannot speak of boundary layers anymore, since the functions $q_2(x), \sigma_{11}(x)$ as given in (13, 14) are non-zero any where in the region between the plates. In this case boundary effects have an important influence on the flow pattern.

Since, at this point, we have no recipe for prescribing all boundary values required, we can not say whether the boundary layers obtained from the R13 equations coincide well with those of the Boltzmann equation. Note that similar problems arise with the Burnett and super-Burnett equations which, however, lead to unphysical oscillations in space [10].

8 Shock structure computations

Now we turn to the non-linear equations. The shock profile connects the equilibrium states of density ρ_0, velocity v_0, and temperature T_0 before the shock at $x \to -\infty$ with the equilibrium ρ_1, v_1, T_1 behind the shock at $x \to \infty$. The process is modeled as one-dimensional flow. Hence, velocity, pressure deviator and heat flux have only one single non-trivial component in the direction normal to the shock wave. The field quantities are related to their values at $x \to -\infty$ by definition of the non-dimensional quantities

$$\hat{\rho} = \frac{\rho}{\rho_0},\ \hat{v} = \frac{v}{\sqrt{RT_0}},\ \hat{T} = \frac{T}{T_0},\ \hat{\sigma} = \frac{\sigma}{\rho_0 RT_0},\ \hat{q} = \frac{q}{\rho_0\sqrt{RT_0}^3},\ \hat{\mu} = \frac{\mu}{\mu_0} = \hat{T}^s\ .$$

As in the linear case, $\hat{\sigma} = \sigma_{\langle 11\rangle}$ represents the non-trivial component of the pressure deviator, called stress in the following, and $\hat{q}$ denotes the normal heat flux.

A dimensionless space variable is introduced as

$$\hat{x} = \frac{x\rho_0\sqrt{RT_0}}{\mu_0}$$

where μ_0 is the viscosity of the state before the shock. From the viscosity follows the mean free path, see e.g. [4] or [2], calculated for $x \to -\infty$, viz.

$$\bar{\lambda}_0 = \frac{4}{5}\frac{\mu_0}{\rho_0\sqrt{\frac{\pi}{8}RT_0}}. \tag{15}$$

Thus, the relation

$$\frac{x}{\bar{\lambda}_0} = \frac{5}{4}\sqrt{\frac{\pi}{8}}\,\hat{x} \approx 0.783\,\hat{x} \tag{16}$$

holds for our dimensionless space variable. In the plots we shall always use x/λ_0 as space variable. For the sake of simplicity we drop the "hats" of non-dimensional variables in the sequel.

The Mach number of the shock

$$M_0 = v_0/\sqrt{\frac{5}{3}}$$

acts as parameter for the computations. Shock structures are formally solutions of the one-dimensional R13 equations with the boundary conditions

$$\text{at } (x \to -\infty): \ \varrho_0 = 1 \ , \ v_0 = \sqrt{\frac{5}{3}} M_0 \ , \ T_0 = 1 \ ,$$

$$\text{at } (x \to \infty): \ \varrho_1 = \frac{\varrho_0 v_0}{v_1} \ , \ v_1 = \sqrt{\frac{5}{3}} \frac{M_0^2 + 3}{4 M_0} \ , \ T_1 = \frac{(5M_0^2 - 1)(M_0^2 + 3)}{16 M_0^2} \ .$$

and $\sigma_0 = \sigma_1 = 0$, $q_0 = q_1 = 0$. The values behind the shock are given by the Rankine-Hugoniot-relations. The density follows from the velocity by means of the mass balance as

$$\rho(v) = \sqrt{\frac{5}{3}} \frac{M_0}{v} \ , \tag{18}$$

and the relations for stress σ and heat flux q as functions of velocity and temperature follow from the conservation laws for momentum and energy as

$$\sigma(v, T) = 1 + \frac{5}{3} M_0^2 - M_0 \sqrt{\frac{5}{3}} \left(\frac{T}{v} + v \right) \tag{19}$$

$$q(v, T) = \sqrt{\frac{5}{12}} M_0 \left(\frac{5}{3} M_0^2 + 5v^2 - 3T \right) - v \left(1 + \frac{5}{3} M_0^2 \right) . \tag{20}$$

The R13 equations were solved by numerically with a method outlined in Ref. [6]. We proceed to discuss the general behavior of shock structure solutions of the R13 equations.

8.1 Transition from Grad's 13-moment-equations

Grad's 13-moment-case was derived as improvement of the NSF theory in the description of rarefied flows. Unfortunately, the equations fail to describe continuous shock structures, since they suffer from a subshock in front of the shock beyond the Mach number $M_0 = 1.65$, see [17] and [18]. This subshock grows with higher Mach numbers and at $M_0 \approx 3.5$ a second subshock appears in the middle of the shock. Both subshocks are artefacts from the hyperbolic nature of the 13-moment equations [40]. It turned out that any hyperbolic moment theory will yield continuous shock structures only up to the Mach number corresponding to the highest characteristic velocity, see [41] and [26]. Further validation of results with measurements shows that moment theories succeed to describe shock thickness data accurately only for Mach numbers far below this critical value. In particular, Grad's 13-moment case describes the shock thickness accurately only up to $M_0 \approx 1.1$. Recent results from [22] required up to 900 moments to calculate a smooth shock structure for $M_0 = 1.8$ that fits to experimental data. For more information on shock structures in moment theories see the textbook [19].

One of the reasons for deriving the regularized 13 moment equations (R13) in [5] was to obtain field equations which lead to smooth and stable shock structures for any Mach number. Since the equations are based on Grad's 13-moment-case, it must be emphasized that physicality of the R13-solutions

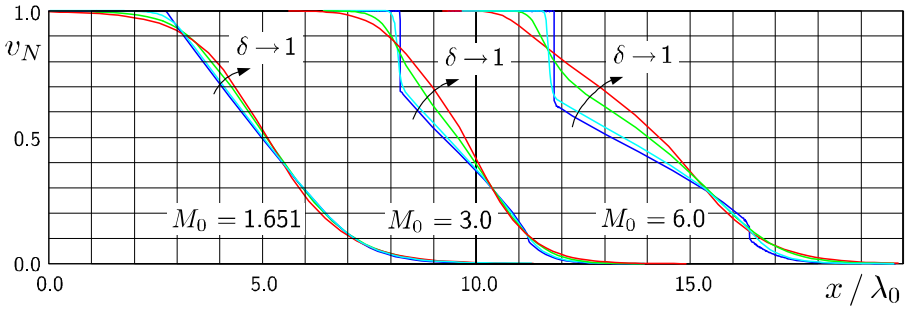

Fig. 3. Regularization process of Grad's 13-moment-equation. Profiles for three different Mach numbers are shown with different values of $\delta = 0.0,\ 0.1,\ 0.5,\ 1.0$. The results of Grad's equation ($\delta = 0$) exhibt kinks as well as up to two subshocks of increasing strength. These singularities vanish in R13 case where $\delta = 1$.

is still restricted to small Mach numbers. However, the range of validity is extended by including higher order expansion terms into the R13 equations.

Fig. 3 shows the transition to smooth shock structures for three different Mach numbers by means of the normalized velocity field v_N. The results are obtained with $s = 1$, i.e. Maxwell molecules. For this, we multiplied the right hand sides of Eqs. (5) with a parameter δ that assumes values between zero and unity. The structures with $\delta = 0$ represent solutions of the classical 13-moment-case, Eqs. (4). For these, at $M_0 = 1.651$ a kink at the beginning of the shock indicates that the highest characteristic velocity is reached before the shock. The kink develops into a pronounced subshock at $M_0 = 3$. In the case $M_0 = 6$ a second subshock is present towards the end of the structure.

The curves for $\delta = 0.1$ follow mainly the results of Grad's 13-moment-case. The subshocks are still clearly visible, albeit smoothed out by increased dissipation.

At $\delta = 1$, however, the additional terms in the regularized 13-moment-equations succeed to completely annihilate the subshocks and an overall smooth shock structure is obtained. At $M_0 = 6$ the R13-solution ($\delta = 1$) exhibits obvious asymmetries which start to appear in the structure with Mach numbers $M_0 > 3$. Since experiments as in [42] or DSMC simulations predict almost perfect s-shaped profiles we conclude that the validity of R13 solutions may be lost beyond Mach numbers $M_0 \approx 3.0$.

8.2 Comparison with DSMC results

In this section we shall compare the shock structures obtained with the R13 equations to the results obtained with the direct simulation Monte-Carlo-method (DSMC) of Bird [4]. For the DSMC results we used the shock structure code which is available from Bird's website. For the actual setup like interval

length, upstream temperature, etc. we adopted the values of Pham-Van-Diep et al. [43]. Note that the calculation of a single low Mach number shock structure by a standard DSMC program takes several hours which is several orders of magnitude slower than the calculation with a continuum model.

We compare to DSMC solutions for Maxwell molecules, computed with Bird's code, see [4]. Since the DSMC code uses physical units we fixed the mean free path of the upstream region λ_0 as $\lambda_0 = 0.0014\,\mathrm{m}$, which corresponds to our definition (15) and also reproduces the shock thickness results of [43].

In the next figures we compare the profiles of density and heat flux. The heat flux in a shock wave follows solely from the temperature and velocity via the relation (20). Hence, its profile gives a combined impression of the quality of the temperature and velocity profile. The soliton-like shape of the heat flux helps also to give a more significant judgement of the quality of the structure. Since it is a higher moment the heat flux is more difficult to match than the stress. We suppress the profiles of velocity, temperature and stress in the following. The density is normalized to give values between zero and unity for each Mach number. Similarly, the heat flux is normalized such that the DSMC result gives a maximal heat flux of 0.9.

Before we present the results of the regularized 13-moment-equations we discuss briefly the failure of the classical theories and the standard Burnett models. Fig. 4 shows the density and heat flux profile of a $M_0 = 2$ shock calculated with the NSF and Grad's 13-moment-system as well as with the Burnett and super-Burnett equations. The NSF results simply mismatches the profile, while the Grad13 solution shows a strong subshock. Burnett and super-Burnett solutions are spoiled by oscillations in the back of the shock.

In the Burnett case the oscillations arise if the length of a grid cell is below half of the mean free path. This is in correspondence to the result of the linear analysis which predicts spatial instabilities. It also explains the appearance of the oscillations in the downstream region, because the mean free path is smaller in that region. Since the oscillations stick to a wave length corresponding to the length of a grid cell, high resolution calculations are impossible. The super-Burnett result shows the same behavior, however the oscillation wave length is a multiple of the length of a grid cell. Still, the oscillations increase with grid refinement and convergence can not be established.

The oscillations of both models, Burnett and super-Burnett, increase for shocks with higher Mach number and are also present for other values of the viscosity exponent. Hence, for the description of shock structures the Burnett-equations and super-Burnett-equations have to be rejected.

Fig. 5 shows shock structures for the Mach numbers $M_0 = 1.5,\ 2,\ 3,\ 4$ calculated with the R13 equations, displayed together with the DSMC results. For smaller Mach numbers the shape of the heat flux is captured very well by the R13 equations, and the density profiles exhibit no visible differences to DSMC. The deviations from DSMC solutions become more pronounced for higher Mach numbers. The R13 results begin to deviate from the DSMC solution in the upstream part.

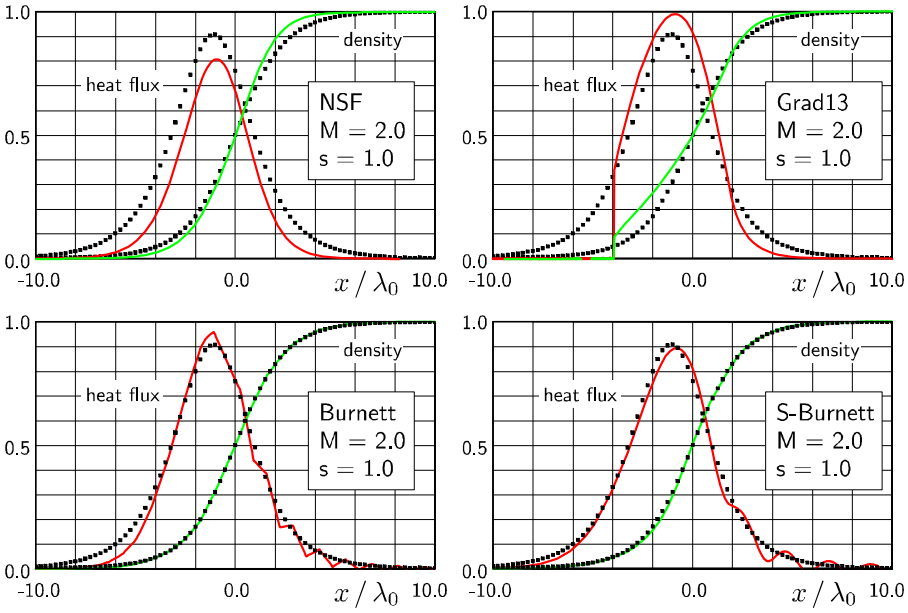

Fig. 4. Shock structure solutions of the system of Navier-Stokes-Fourier, the classical 13 moment case of Grad, and Burnett and super-Burnett-equations for Maxwell molecules at Mach number $M_0 = 2$ (solid lines). Both Burnett results exhibit non-physical oscillations in the downstream region. The squares represent the DSMC solution.

From the presented figures we may conclude that the results of the R13 system for Maxwell molecules agree well with DSMC results. For higher Mach numbers, however, the R13 equations deviate from DSMC data, and the applicability of the theory is no longer given, when quantitative features are needed to be captured.

9 Conclusions

We conslude that the R13 equations are superior to all competing models, i.e. Burnett and super-Burnett equations, models derived thereof, and Grad's 13 moment equations. They are unconditionally stable, and stand in good agreement with experiments for dispersion and damping, and shock structures. The equations discussed above are derived for the special case of Maxwell molecules. Other molecular interaction models can be incorporated ad hoc by adjusting the viscosity coefficient s in Eq. (6). However, the proper derivation is discussed in Ref. [36] where it becomes clear that more than 13 moments will be needed for a proper third order theory for non-Maxwellian molecules.

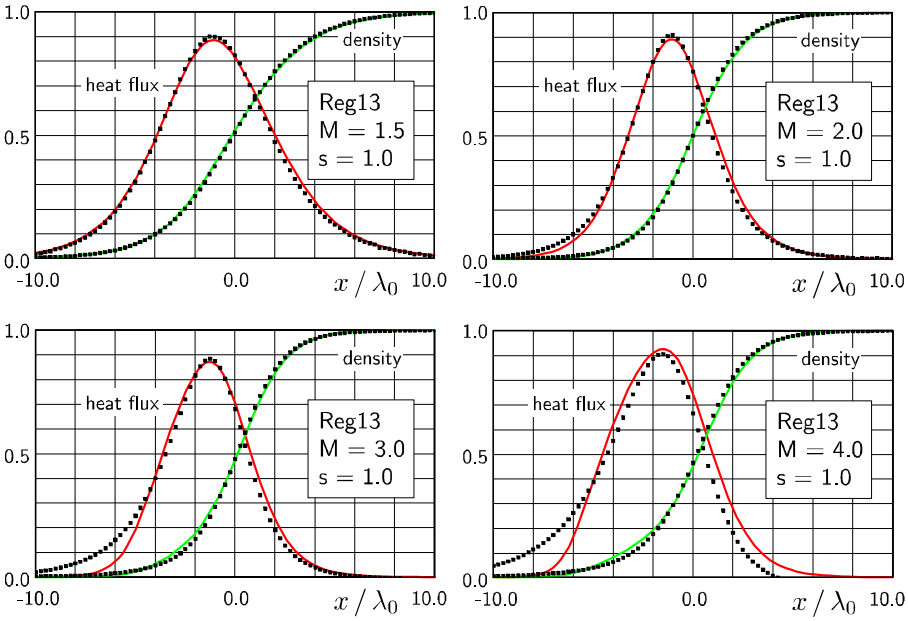

Fig. 5. Shock structures in a gas of Maxwell molecules with Mach numbers $M_0 = 1.5, 2.0, 3.0, 4.0$. Solid lines show the solution of the R13 equations, while squares correspond to the DSMC solution.

The most pressing question at present is to find proper boundary conditions for the R13 equations, and we hope to be able to present these in the future.

Acknowledgement. This research was supported by the Natural Sciences and Engineering Research Council (NSERC).

References

1. C. Cercignani, *Theory and application of the Boltzmann Equation.* Scottish Academic Press, Edinburgh 1975
2. S. Chapman and T. G. Cowling, *The mathematical Theory of Non-Uniform Gases.* Cambridge University Press 1970
3. T. Ohwada *Heat flow and temperature and density distributions in a rarefied gas between parallel plates with different temperatures. Finite difference analysis of the nonlinear Boltzmann equation for hard sphere molecules.* Phys. Fluids **8**, 2153-2160 (1996)
4. G. Bird, *Molecular gas dynamics and the direct simulation of gas flows.* Clarendon Press, Oxford 1994
5. Struchtrup, H. and Torrilhon, M., *Regularization of Grad's 13-moment-equations: Derivation and Linear Analysis,* Phys. Fluids **15**/9, (2003) p.2668

6. M. Torrilhon, and H. Struchtrup, *Smooth Shock Structures for High Mach Numbers with Regularized 13-Moment-Equations*, submitted 2002
7. J.H. Ferziger and H.G. Kaper, *Mathematical theory of transport processes in gases.* North-Holland, Amsterdam 1972
8. A.V. Bobylev, *The Chapman-Enskog and Grad methods for solving the Boltzmann equation.* Sov. Phys. Dokl. **27**, 29-31 (1982)
9. M.Sh. Shavaliyev, *Super-Burnett Corrections to the Stress Tensor and the Heat Flux in a Gas of Maxwellian Molecules.* J. Appl.Maths. Mechs. **57**(3), 573-576 (1993)
10. H. Struchtrup, *Failures of the Burnett and Super-Burnett equations in steady state processes*, submitted (2003)
11. I.V. Karlin , and A.N. Gorban, Hydrodynamics from Grad's equations: What can we learn from exact solutions?, Ann. Phys.-Berlin **11** (10-11): 783-833 (2002)
12. Zheng, Y. and Struchtrup, H., *Burnett equations for the ellipsoidal statistical BGK Model,* accepted for publication in Cont. Mech. Thermodyn (2003)
13. Zhong, X., MacCormack, R.W., and Chapman, D.R., *Stabilization of the Burnett Equations and Applications to High-Altitude Hypersonic Flows,* AIAA 91-0770 (1991)
14. Zhong, X., MacCormack, R. W., and Chapman, D. R., *Stabilization of the Burnett Equations and Applications to Hypersonic Flows,* AIAA Journal **31**, (1993) p.1036
15. S. Jin and M. Slemrod, *Regularization of the Burnett equations via relaxation.* J. Stat. Phys. **103** (5-6), 1009-1033 (2001)
16. S. Jin, L. Pareschi, and M. Slemrod, *A Relaxation Scheme for Solving the Boltzmann Equation Based on the Chapman-Enskog Expansion,* Acta Mathematicas Applicatae Sinica (English Series) **18**, 37-62, 2002.
17. H. Grad, *On the Kinetic Theory of Rarefied Gases.* Comm. Pure Appl. Math. **2**, 325 (1949)
18. Grad, H.: *Principles of the Kinetic Theory of Gases*, in Handbuch der Physik, editor S. Flügge, Springer, Berlin (1958), vol. 12
19. I. Müller and T. Ruggeri, *Rational Extended Thermodynamics.* Springer, New York 1998 (Springer Tracts in Natural Philosophy Vol. 37)
20. H. Struchtrup *Heat Transfer in the Transition Regime: Solution of Boundary Value Problems for Grad's Moment Equations via Kinetic Schemes.* Phys. Rev. E **65**, 041204 (2002)
21. H. Struchtrup, *An Extended Moment Method in Radiative Transfer: The Matrices of Mean Absorption and Scattering Coefficients.* Ann. Phys. **257**, 111-135 (1997)
22. J.D. Au, *Nichtlineare Probleme und Lösungen in der Erweiterten Thermodynamik.* Dissertation, Technical University Berlin 2000
23. J. D. Au, M. Torrilhon, and W. Weiss, *The Shock Tube Study in Extended Thermodynamics*, Phys. Fluids **13**(8), 2423-2432 , (2001)
24. H. Struchtrup, *Kinetic schemes and boundary conditions for moment equations.* ZAMP **51**, 346-365 (2000)
25. H. Struchtrup, *Some remarks on the equations of Burnett and Grad.* IMA Volume **135** "Transport in Transition Regimes", Springer, New York (in press)
26. W. Weiss, *Continuous shock structure in extended Thermodynamics.* Phys. Rev. E **52**, 5760 (1995)
27. D. Reitebuch and W. Weiss, *Application of High Moment Theory to the Plane Couette Flow.* Cont. Mech. Thermodyn. **11**, 227 (1999)

28. H. Struchtrup, *Grad's Moment Equations for Microscale Flows,* Symposium on Rarefied Gasdynamics 23, AIP Conference Proceedings 663, 792-799 (2003)
29. E. Ikenberry and C. Truesdell, *On the pressures and the flux of energy in a gas according to Maxwell's kinetic theory I.* J. of Rat. Mech. Anal. **5**, 1-54 (1956)
30. C. Truesdell and R.G. Muncaster, *Fundamentals of Maxwell's kinetic theory of a simple monatomic gas.* Academic Press, New Yorck 1980
31. S. Reinecke and G.M. Kremer, *Method of Moments of Grad.* Phys. Rev. A **42** , 815-820 (1990)
32. S. Reinecke and G.M. Kremer, *Burnett's equations from a (13+9N)-field theory.* Cont Mech. Thermodyn. **8**, 121-130 (1996)
33. I.V. Karlin, A.N. Gorban, G. Dukek, and T.F. Nonnenmacher, *Dynamic correction to moment approximations*, Phys. Rev. E, 57(2), 1668-1672 (1998)
34. D.Serre, *Systems of Conservation Laws (vol.1)*, Cambridge Univ. Press, Cambridge (1999)
35. S. Jin, and Z.P.Xin, *The Relaxation Schemes for Systems of Conservation Laws in Arbitrary Space Dimensions*, Comm. Pure Appl. Math. **48** (3): 235-276 (1995)
36. H. Struchtrup, *Stable transport equations for rarefied gases at high orders in the Knudsen number*, submitted (2003)
37. I. Müller, D. Reitebuch, and W. Weiss, *Extended Thermodynamics - Consistent in Order of Magnitude*, Cont. Mech. Thermodyn. **15**, 113-146 (2003)
38. P.L. Bhatnagar, E.P. Gross and M. Krook, *A Model for collision processes in gases. I. Small Amplitude Processes in Charged and Neutral One-Component Systems.* Phys.Rev. **94**, 511-525 (1954)
39. E. Meyer, and G. Sessler, *Schallausbreitung in Gasen bei hohen Frequenzen und sehr niedrigen Druecken*, Zeitschr. Physik **149**, 15-39 (1957)
40. Torrilhon, M., *Characteristic Waves and Dissipation in the 13-Moment-Case*, Cont. Mech. Thermodyn. **12**, (2000) p.289
41. Ruggeri, T.: *Breakdown of Shock Wave Structure Solutions*, Phys. Rev. E **47**, (1993)
42. Alsmeyer, H., *Density Profiles in Argon and Nitrogen Shock Waves Measured by the Absorbtion of an Electron Beam*, J. Fluid Mech. **74**/3, (1976) p.497
43. Pham-Van-Diep, G. C., Erwin, D. A., and Muntz, E. P.: *Testing Continuum Descriptions of Low-Mach-Number Shock Structures*, J. Fluid Mech. **232**, (1991) p.403